IEEE Photonics Journal
An IEEE Photonics Society Publication

Open Access

Stress Direction Measurement Based on Polarization State in Optical Fibers Using the Quaternion Method

Volume 9, Number 6, December 2017

Zejia Huang
Chongqing Wu
Zhi Wang

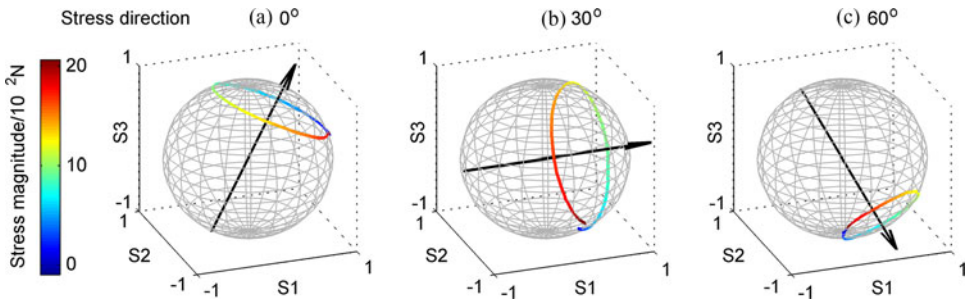

DOI: 10.1109/JPHOT.2017.2764102
1943-0655 © 2017 IEEE

IEEE photonics SOCIETY

IEEE

Stress Direction Measurement Based on Polarization State in Optical Fibers Using the Quaternion Method

Zejia Huang, Chongqing Wu, and Zhi Wang

Key Lab of Education Ministry on Luminescence and Optical Information Technology, Institute of Optical Information, School of Science, Beijing Jiaotong University, Beijing 100044, China

DOI:10.1109/JPHOT.2017.2764102

Manuscript received August 29, 2017; revised October 8, 2017; accepted October 14, 2017. Date of publication October 18, 2017; date of current version November 15, 2017. This work was supported by the National Natural Science Foundation of China under Grants 61775012 and 61571035. Corresponding author: Chongqing Wu (e-mail: cqwu@bjtu.edu.cn).

Abstract: The state of polarization (SOP) in a polarization-maintaining fiber subjected to external stress is studied using the quaternion method. The stress principal axis on the Poincare sphere is independent of intrinsic birefringence, but has a linear relationship with the direction of external stress. The above linear relationship, in turn, enables a measurement of the external stress's direction by calculating the consecutive trajectory of SOP on the Poincare sphere. This method is proposed and experimentally validated by measuring different types of fibers with maximum angle measurement errors of less than 2.24%.

Index Terms: Birefringence quaternion, polarization-maintaining fibers, fiber optics sensor, fiber stress measurement.

1. Introduction

Polarization maintaining fiber (PMF) is a kind of fiber that maintains the state of polarization (SOP) during propagation without distortion. PMF has been attracting intensive research in the field of optical fiber communication and optical fiber sensing for several decades, which attributes to its anti-interference and polarization-maintaining characteristics. Up to now, PMF has been widely used in optical fiber sensors to measure parameters such as vibration [1], [2], stress [3], temperature [4], birefringence [5], [6], bending [7], beat-length [8], etc. The SOP in PMF depends on the intrinsic birefringence, temperature, stress, fiber laying state (twisting, bending, etc.). Among them, the external stress is an important reason that deteriorates the polarization maintaining performance, since it is random, distributed and uncertain in practical application. However, the changes of SOP in PMF induced by external stress are still undefined in detail so far. Thus, as a research stage, it is necessary to exclude the impact of temperature and fiber laying state, and to study the changes of SOP in fibers that subjected to external stress alone.

The birefringence of PMF induced by stress has been studied for a long time. Based on the study of birefringence induced by stress in single-mode fiber (SMF) [9], [10], Chu and Sammut calculated the stress birefringence and material birefringence of PMF [11] in 1984. In [12] by Tsubokawa *et al.*, the mode coupling of PMF caused by stress was analyzed in-depth, which had laid the foundation for distributed stress measurement based on PMF. In 1979, Ulrich, Simon and Johnson presented that elliptical birefringence results from the superposition of linear and circular

birefringence, because the corresponding rotations are infinitesimal, they commute and can simply be added vectorially [13], [14]. In the same year, Rashleigh and Ulrich presented in [15] that the total birefringence of general fiber consists of inherent, bending, twisting and magnetic birefringence, and the superimposed birefringence axis satisfies the principle of vector superposition in Stokes space. In particular, if the main axis of geometric birefringence and stress birefringence are consistent, they can be simply added [16]–[19]. The conclusion that the addition of different birefringence satisfies the principle of vector superposition has been stated in many papers for years. However, virtually no paper shows why the total birefringence satisfies the principle of vector superposition and under what conditions. In fact, it is very complicated to prove it by traditional Jones-Mueller matrix. Thus, in this paper we will prove this conclusion using a much simpler method, the quaternion method.

Recently, many innovative technologies have been employed to fulfill the stress sensing based on PMFs, such as polarization optical time-domain reflectometer (P-OTDR) [3], Brillouin dynamic gratings [20], Sagnac interferometer [21], etc. Meanwhile, the stress distribution and stress birefringence of PMF are still research topics of large interest [3], [5], [22]. However, most reports about optical fibers stress sensors are only focusing on the stress magnitude measurement [23] but neglecting the measurement of stress direction. If the stress direction measurement capability based on optical fibers could be provided, the optical fibers stress sensors are able to be employed in more practical applications.

Up to now, Mueller matrix and Jones matrix have been used widely to study the polarization phenomena in optical fibers. Considering the algorithmic complexity of matrixes, some researchers have used quaternion to analyze the SOP in optical fibers [24], [25]. Furthermore, the SOP quaternion was redefined in [26] and [27], the quaternion method to describe the SOP of light and the polarized optical components and systems were theoretically derived based on the Poincare sphere and quaternion representations. As we will show analytically in Section 2, the quaternion that corresponds to Jones and Mueller matrix (Jones-Mueller quaternion-JMQ) employed in this paper is sufficient to simplify the treatment of polarization phenomena as well as the calculation work.

In this paper, JMQ is utilized as a mathematical tool to describe the evolution of SOP induced by stress in PMF. In Section 2, we prove the principle of birefringence vector superposition using the quaternion method. Furthermore, we study the impact of external stress on the SOP of transmission light in PMF by using JMQ, and propose the linear relationship between the external stress direction and the stress principal axis. In Section 3, a bow-tie Hi-Bi PMF, a G.652 SMF and a Spun Hi-Bi PMF are employed respectively to measure the external stress direction based on the linear relationship proposed in Section 2, with maximum angle measurement error of 2.24%. The experimental results reveal that not only PMF, but also fibers showing low birefringence, such as SMF are capable to realize the measurement of stress direction with low measurement error.

2. Theory Analysis

2.1 Birefringence Superposition

A Mueller quaternion (represented by Edwardian Script ITC font) in exponential form can be used to denote all polarizing properties of a fiber, which is defined as [27]

$$\mathscr{U} = \exp(\mathscr{A}) = \exp\left[-\bar{\alpha}/2 + \mathrm{i}\bar{\varphi}/2 + \hat{\boldsymbol{n}}(\Delta\varphi/2 - \mathrm{i}\Delta\alpha/2)\right] \tag{1}$$

Where the scalar part $-\bar{\alpha}/2 + i\bar{\varphi}/2$ denotes the polarization independent power transmission, its real component $-\bar{\alpha}/2$ and imaginary component $\mathrm{i}\bar{\varphi}/2$ denote the polarization-independent loss and polarization-independent phase shift respectively. The vector part $\hat{\boldsymbol{n}}(\Delta\varphi/2 - \mathrm{i}\Delta\alpha/2)$ denotes the polarization dependent power transmission, its real component $\hat{\boldsymbol{n}}\Delta\varphi/2$ and imaginary component $-\hat{\boldsymbol{n}}\,\mathrm{i}\Delta\alpha/2$ denote the polarization-dependent phase shift and polarization-dependent loss respectively. The unit vector $\hat{\boldsymbol{n}}$ is the principal axis of birefringence. The SOP along the fiber is related to the phase shift and loss. Since the length of fiber under test (FUT) in the next experimental section is rather short, the loss of fiber is small enough to be neglected. Thus in this paper we only take the phase shift into account, which mainly leads to the changes of SOP along the fiber, the quaternion

$\mathscr{A}$ in Eq. (1) can be simplified as

$$\mathscr{A} = \mathrm{i}\bar{\varphi}/2 + \hat{\boldsymbol{n}}\ \Delta\varphi/2 = \mathrm{i}\bar{\beta}L\ + \hat{\boldsymbol{n}}\Delta\beta L \tag{2}$$

Where $\bar{\beta}$ is the average propagation constant which can be treated as a constant, L denotes the length of the FUT, and the propagation constant difference between the fast and slow axis of PMF is denoted by $\Delta\beta$.

In a stress-induced high-birefringence PMF (e.g., bow-tie Hi-Bi PMF), the internal stress is the main factor that determines the polarization maintaining properties of the fiber. If the FUT is also subjected to external stress, then we need to consider the impact of both internal and external stress on the dielectric constant. By using perturbation approximation, the dielectric constant can be described as

$$\begin{pmatrix} \varepsilon_{xx} & \varepsilon_{xy} & \varepsilon_{xz} \\ \varepsilon_{yx} & \varepsilon_{yy} & \varepsilon_{xz} \\ \varepsilon_{zx} & \varepsilon_{zy} & \varepsilon_{zz} \end{pmatrix}(x, y, z) = \varepsilon_{\mathrm{ina}}(x, y, z)\boldsymbol{I}\ + \boldsymbol{C}\boldsymbol{\sigma}_{\mathrm{int}}(x, y, z) + \boldsymbol{C}\boldsymbol{\sigma}_{\mathrm{ext}}(x, y, z) \tag{3}$$

The left side of Eq. (3) denotes that the dielectric constant of a fiber that subjected to stress will change from isotropy to anisotropy due to the elasto-optic effect, whether the stress comes from inside or outside the fiber. The first term of the right side $\varepsilon_{\mathrm{ina}}(x, y, z)\boldsymbol{I}$ denotes the dielectric property without stress (i.e., the geometric dielectric constant), where $\boldsymbol{I}$ is a 3×3 unit matrix. In a stress-induced PMF, the core is approximately circular and this term is much smaller than the stress dielectric constant, thus this term is neglected in the following sections. The second term $\boldsymbol{C}\boldsymbol{\sigma}_{\mathrm{int}}(x, y, z)$ represents the changes of refractive index due to internal stress. In practical terms, the birefringence $\Delta\varepsilon$ between two orthogonal modes of LP_{01} can be measured experimentally. If only the changes in the cross-section are considered, this term can be written as a form independent of the profile (x, y)

$$\boldsymbol{C}\boldsymbol{\sigma}_{\mathrm{int}}(x, y) = \begin{bmatrix} \Delta\varepsilon & 0 \\ 0 & -\Delta\varepsilon \end{bmatrix} \tag{4}$$

The third term $\boldsymbol{C}\boldsymbol{\sigma}_{\mathrm{ext}}(x, y, z)$ represents the changes of refractive index due to external stress. In this paper, we ignore the impact of external stress on the internal stress zone of a stress-induced PMF, only consider the direct impact of external stress on the refractive index distribution. Moreover, since the longitudinal variation of refractive index usually does not contribute to the birefringence, so only the changes in the cross-section is taken into account, thus this term can be expressed in the external stress coordinate system $\xi O \eta$

$$\boldsymbol{C}\boldsymbol{\sigma}_{\mathrm{ext}}(\xi, \eta) = \begin{bmatrix} \varepsilon'_{\xi\xi} & \varepsilon'_{\xi\eta} \\ \varepsilon'_{\eta\xi} & \varepsilon'_{\eta\eta} \end{bmatrix}(\xi, \eta) = \begin{bmatrix} \bar{C}(\bar{\sigma}_{\xi\xi} + \bar{\sigma}_{\eta\eta}) + \Delta C(\bar{\sigma}_{\xi\xi} - \bar{\sigma}_{\eta\eta}) & 0 \\ 0 & \bar{C}(\bar{\sigma}_{\xi\xi} + \bar{\sigma}_{\eta\eta}) - \Delta C(\bar{\sigma}_{\xi\xi} - \bar{\sigma}_{\eta\eta}) \end{bmatrix} \tag{5}$$

The derivation process and symbolic representations of Eq. (5) are given in Appendix. Since the relationship between the refractive index n and the dielectric constant ε can be written as $n = \varepsilon^{1/2}$, Eq. (3)–(5) can be transformed approximately to the form of refractive index quaternion, written as

$$\mathscr{N}_{\mathrm{total}} = \mathscr{N}_{\mathrm{int}} + \mathscr{N}_{\mathrm{ext}} \tag{6}$$

Where the total refractive index $\mathscr{N}_{\mathrm{total}} = n_{\mathrm{total}} + \boldsymbol{N}_{\mathrm{total}}$. Similarly, the refractive index induced by the internal and external stress are given by $\mathscr{N}_{\mathrm{int}} = n_{\mathrm{int}} + \boldsymbol{N}_{\mathrm{int}}$ and $\mathscr{N}_{\mathrm{ext}} = n_{\mathrm{ext}} + \boldsymbol{N}_{\mathrm{ext}}$ respectively. Thus Eq. (6) can be written in the form of quaternion

$$n_{\mathrm{total}} + \boldsymbol{N}_{\mathrm{total}} = n_{\mathrm{int}} + \boldsymbol{N}_{\mathrm{int}} + n_{\mathrm{ext}} + \boldsymbol{N}_{\mathrm{ext}} \tag{7}$$

According to the equality rule of quaternions, Eq. (7) can be decomposed into a scalar equation and a vector equation as

$$n_{\mathrm{total}} = n_{\mathrm{int}} + n_{\mathrm{ext}} \tag{8}$$

$$\boldsymbol{N}_{\mathrm{total}} = \boldsymbol{N}_{\mathrm{int}} + \boldsymbol{N}_{\mathrm{ext}} \tag{9}$$

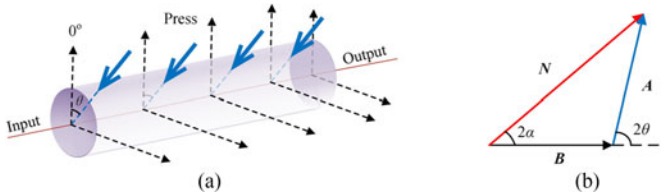

Fig. 1. (a) The squeezed PMF. (b) The addition of vector in Stokes space.

Since the vector part of refractive index quaternion $\mathscr{N}$ denotes the polarization-dependent phase shift, thus the vector equation (9) denotes the superposition of birefringence vector. In another word, the sum of birefringence satisfies the principle of vector superposition, once the sum of dielectric constant can be written in the form of Eq. (3). The whole derivation process can be summed up as: if the dielectric constant can be added in the form of Eq. (3), then the refractive index quaternion satisfies the superposition principle approximately. Since the vector part of the refractive index quaternion is birefringence, as a result, the birefringence satisfies the principle of vector superposition.

2.2 The Influence of External Stress Direction

As shown in Fig. 1(a), the PMF is subjected to external stress in the direction of θ with respect to the orientation of the intrinsic principal axis (i.e., the fast or slow axis of PMF). The combined impact of the internal and external stress creates a new principal axis of birefringence, whose orientation is different from the intrinsic one. Only consider the birefringence (i.e., the vector part of the quaternion in Eq. (2)), the polarizing property of the fiber is assumed to be given by a simplified quaternion

$$e^{\boldsymbol{N}} = e^{\hat{\boldsymbol{n}}(\alpha)\Delta\beta L} \tag{10}$$

Where α is the angle between the intrinsic and the new principal axis of birefringence $\hat{\boldsymbol{n}}$; $\Delta\beta$ is the propagation constant difference after squeezing; L is the squeezed section length. In Stokes space shown in Fig. 1(b), constant vector $\boldsymbol{B}$ is the intrinsic birefringence of the squeezed fiber; vector $\boldsymbol{A} = \hat{\boldsymbol{n}}(2\theta)kp$ is the birefringence induced by external stress, where p is the magnitude of external stress, $\hat{\boldsymbol{n}}(2\theta)$ and θ are the unit vector and direction of external stress respectively. The constant k, which can be measured by experiment [23], is dependent on the elasto-optical coefficient but independent of the intrinsic birefringence. The vector sum $\boldsymbol{N}$ is the total birefringence of the squeezed fiber, it can be written as follow according to Eq. (9)

$$\boldsymbol{N} = \boldsymbol{B} + \boldsymbol{A} \tag{11}$$

Since the intrinsic birefringence is definite, the total birefringence of the squeezed fiber only varies with the direction θ and magnitude p of the external stress.

Thus, the polarizing property of the entire PMF in Fig. 1(a) can be represented by a JMQ as

$$e^{\boldsymbol{N}} = e^{\boldsymbol{B}+\boldsymbol{A}} \tag{12}$$

The SOP quaternion of the input light $\mathscr{S}_{\text{in}}$ and output light $\mathscr{S}_{\text{out}}$ in Fig. 1(a) now can be expressed as

$$\mathscr{S}_{\text{out}} = e^{\boldsymbol{N}/2}\mathscr{S}_{\text{in}}e^{-\boldsymbol{N}/2} \tag{13}$$

Substituting Eq. (12) into Eq. (13), the SOP of the output light can be written as

$$\mathscr{S}_{\text{out}} = e^{(\boldsymbol{B}+\boldsymbol{A})/2}\mathscr{S}_{\text{in}}e^{-(\boldsymbol{B}+\boldsymbol{A})/2} = e^{[\boldsymbol{B}+\hat{\boldsymbol{n}}(2\theta)kp]/2}\mathscr{S}_{\text{in}}e^{-[\boldsymbol{B}+\hat{\boldsymbol{n}}(2\theta)kp]/2} \tag{14}$$

According to the rule of quaternions product [22] (note that this product rule is slightly different from the conventional product rule.), the differential of $\mathscr{S}_{\text{out}}$ with respect to p can be written as the

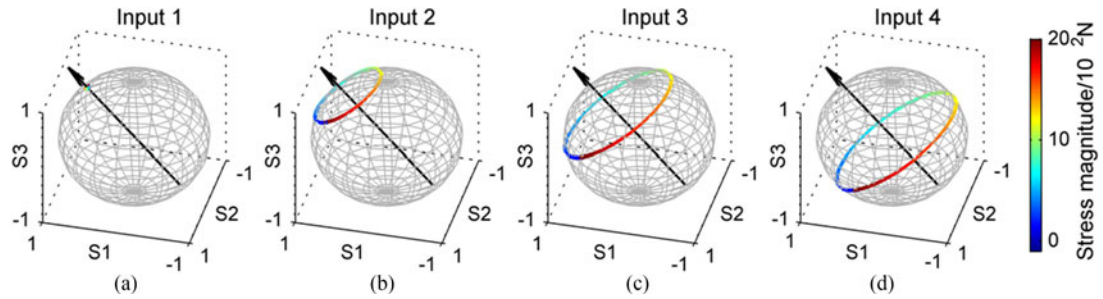

Fig. 2. (a)–(d) respectively corresponds to different SOP of incident light. The gradient circle on the Poincare sphere is the SOP of the output light that changes with the magnitude of external stress. The black arrow vector is the rotation axis of the circle, namely, the stress principal axis.

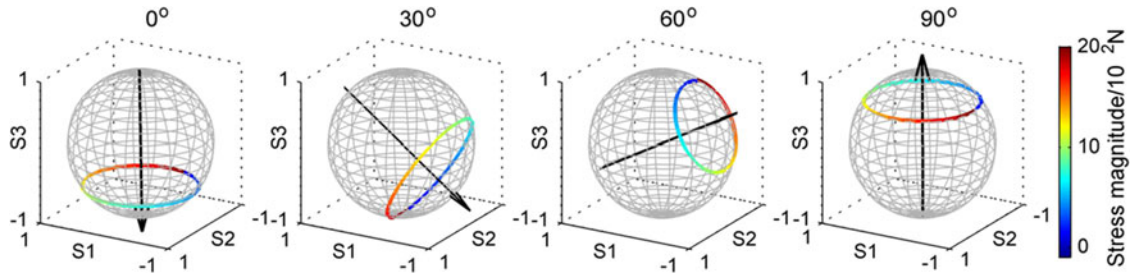

Fig. 3. The subfigures respectively show the shift of stress principal axis, when the direction of external stress changes from 0° to 90°. The gradient circle is the SOP of output light that changes with the magnitude of external stress. The black arrow vector is the stress principal axis.

cross product of two vectors,

$$\frac{\partial \mathscr{S}_{\text{out}}}{\partial p} = \frac{1}{2}[\hat{\boldsymbol{n}}(2\theta)k\mathscr{S}_{\text{out}} - \mathscr{S}_{\text{out}}(\hat{\boldsymbol{n}}(2\theta)k)] = \hat{\boldsymbol{n}}(2\theta)k \times \boldsymbol{S}_{\text{out}} \tag{15}$$

Where quaternion $\mathscr{S}_{\text{out}} = s_{\text{out}} + \boldsymbol{S}_{\text{out}}$, substituting this equation into Eq. (15), the expressions describe the SOP of the output light in a PMF subjected to external stress is finally derived as

$$\partial s_{\text{out}}/\partial p = 0 \tag{16}$$

$$\partial \boldsymbol{S}_{\text{out}}/\partial p = \hat{\boldsymbol{n}}(2\theta)k \times \boldsymbol{S}_{\text{out}} \tag{17}$$

According to Eq. (16)–(17), the SOP of output light is depicted in Fig. 2 for different input SOP. A conclusion can be drawn that, the variation of the external stress magnitude p will cause the vector $\boldsymbol{S}_{\text{out}}$ rotates around the stress principal axis $\hat{\boldsymbol{n}}(2\theta)$ with a certain angular rate k and draws closed circles on the Poincare sphere. Note that the stress principal axis is different from the principal axis of birefringence in Eq. (10). Although similar conclusions were obtained using coupled mode theory and Mueller matrix method [23], [28]; but by using the quaternion method, the derivation process is much more simply and directly. Moreover, the relationship between the stress principal axis and external stress direction is apparently shown in Eq. (17), while it is impossible to derive this relationship by traditional method because the Mueller matrix does not contains any stress direction information.

As shown in Eq. (17), the stress principal axis $\hat{\boldsymbol{n}}(2\theta)$ depends on the direction of external stress θ, which is depicted in Fig. 3, the variation of the stress principal axis direction in Stokes space is twice the external stress direction in three-dimensional space. The fact that the azimuths on the Poincare sphere are twice those of the real space is stated in [29] by Ramachandran and Ramaseshan in 1961. Obviously, it is easy to calculate the stress principal axis based on the SOP of the output light on the Poincare sphere. Since there is a twice linear relationship between the direction of

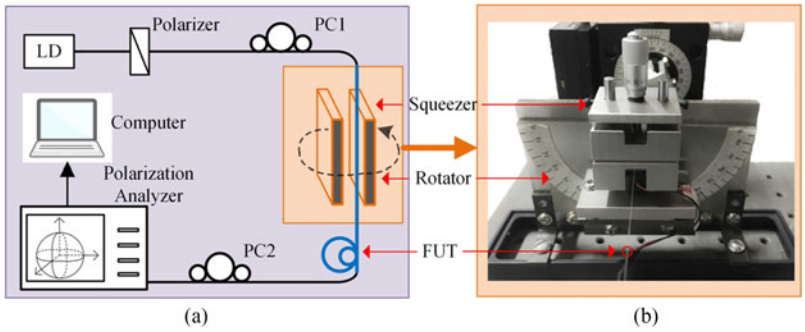

Fig. 4. (a) Experimental setup. (b) Rotatable fiber squeezer and six-dimensional fine-tuning frame. LD: laser diode. PC: polarization controller.

external stress and the direction of stress principal axis, it seems feasible to measure the direction of external stress directly from the SOP information of the output light. Thus we will apply this method to measure the direction of external stress and verify whether it is efficient and accurate enough for practical applications.

3. Experiment

3.1 Experimental Setup

Before the experiment, the ways of rotating the external stress direction are required to be explained firstly. There are two ways to change the direction, rotate the fiber or rotate the stress around the longitudinal axis of the fiber. If the FUT are rotated longitudinal (twisted), the principal axis of polarization in PMF will change even without external stress, ultimately lead to undesired mode coupling, which could be expected to induce measurement error. Thus in this experiment the FUT remains fixed, the direction of external stress is changed by rotating the squeezer, which squeezes the fibers in opposite sides of the fibers. This method would provide higher reliability and stability to the measurement.

The experimental setup used to validate the measurement method is shown in Fig. 4. Continuous wave with controllable polarizations are launched into the squeezed fiber, then the SOP of the output light are acquired and transmitted to computer.

A distributed-feedback (DFB) laser operating at 1544 nm from CONOUER Corp is used to generate high extinction ratio continuous wave. Since the scheme basically requires the generation of continuous wave having controllable polarization, a polarization controller PC1 is utilized to change the SOP of incident light. Then the polarized light is launched into the FUT, which through the center of the fiber squeezer with a squeezed length of 0.03 m. The FUT are a 1 m long bow-tie PMF from Beijing Glass Research Institute (BGRI), a 1 m long G.652 SMF and 1 m long Spun Hi-Bi PMF from Yangtze Optical Fiber and Cable Corp (YOFC) respectively. Considering that any movement of the FUT during the experiment will reduce the measurement accuracy, thus both ends of the FUT are fixed and straightened by two six-dimensional fine-tuning frames, which are fixed on the optical platform. The fiber squeezer in Fig. 4(b) is installed on a customized rotator, which can be accurately rotated around the fiber longitudinal axis from 0° to 180° with steps of 1°. The squeezer is equipped with linear bearings to ensure the parallel movement of the squeezer components and the average distribution of stress. A Piezoelectric Transducer (PZT), driven by voltage (from 0 V to 150 V) and installed on the squeezer, is used to modulate the magnitude of external stress. Considering that it is complicated to align the given external stress direction with one of the intrinsic principal axis of birefringence in FUT every time, we choose a separate reference coordinate systems for the external stress direction. Thus, in the following experiments we use the relative direction to denote the direction of external stress, which in fact does not affect

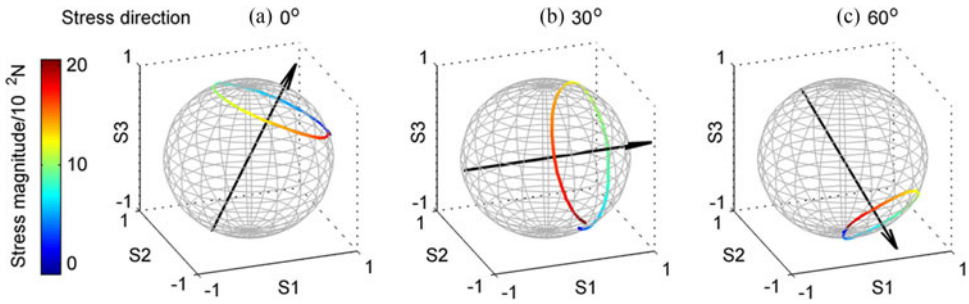

Fig. 5. The FUT is a bow-tie PMF, the subfigures respectively show the change of stress principal axis, when the direction of external stress changes from 0° to 60°. The gradient circle is the traces of the output SOP that changes with the magnitude of external stress. The black arrow vector is the stress principal axis.

the measurement results according to the analysis in Section 2. The PC2 is actually not essential for this scheme, but it help to simplify data processing by locating the initial SOP (i.e., when the external stress is zero) of the output light in specific positions on the Poincare sphere. At the receiver end, the SOP of the output light is acquired by a polarization analyzer from General Photonics Corp and then processed by a computer.

3.2 Experimental Results and Discussions

Using the setup depicted in Fig. 4, the bow-tie PMF is placed in the center of the squeezer, the rotator is rotated around the core of fiber, which means the external stress direction is changed with respect to the intrinsic principal axis of birefringence. After continuously increasing the voltage of PZT, the PMF is squeezed, resulting in the consecutive movement of output SOP on the Poincare sphere. Rotate the rotator in different direction and then record the respective SOP traces. The SOP of the output light acquired are depicted in Fig. 5, while the external stress is directed in the direction of 0°, 30° and 60° respectively. Under this condition, the stress principal axis shift apparently with the direction of external stress, and the variation of the principal axis direction are approximately twice the external stress direction. The depicted experiment results in Fig. 5 validate the proposed method in Section 2 is feasible to measure the stress direction using bow-tie PMF (or stress-induced high birefringence optical fibers).

It is worth mentioning that since the loss of the optical fiber in the experiment is existent, it will slightly change the output SOP. Thus the SOP's circles obtained from the experiment are not closed as the circles in Fig. 3 (in that section the loss is neglected).

Although the theoretical conclusion in Section 2 are derived from linear Hi-Bi PMF, while the conclusion denotes that the changes of stress principal axis are independent of the intrinsic birefringence. Which means that for most types of fiber, we wound still get similar results to the ones shown in Fig. 5. Thus in the next step we will verify experimentally whether this measurement method is equally applicable to the other types of fiber.

Repeat the same above experimental procedure of Fig. 4, while replace the FUT, the SOP of the output light with different external stress direction are depicted in Figs. 6 and 7, where the FUT are a Spun Hi-Bi PMF (i.e., high polarization mode coupling fiber) and a G.652 SMF respectively. No matter what types of fiber we used, the SOP of the output light rotates around the stress principal axis, and the stress principal axis changes with the direction of external stress. Moreover, the variation of the principal axis direction are approximately twice the direction of external stress. Special attention should be paid to the SOP of the Spun Hi-Bi PMF in Fig. 6, which are not so closed as the other two in Figs. 5 and 7, since the loss of this Spun Hi-Bi PMF is greater than the other two, hence it causes greater effect to the polarization state. In addition to this difference, the similar behaviors shown from the above experiment results reveal that the method employed to

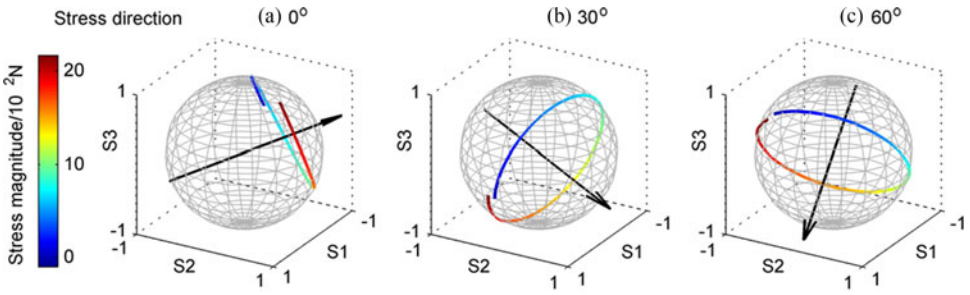

Fig. 6. The FUT is a Spun Hi-Bi PMF, the subfigures respectively show the change of stress principal axis when the direction of external stress changes from 0° to 60°.

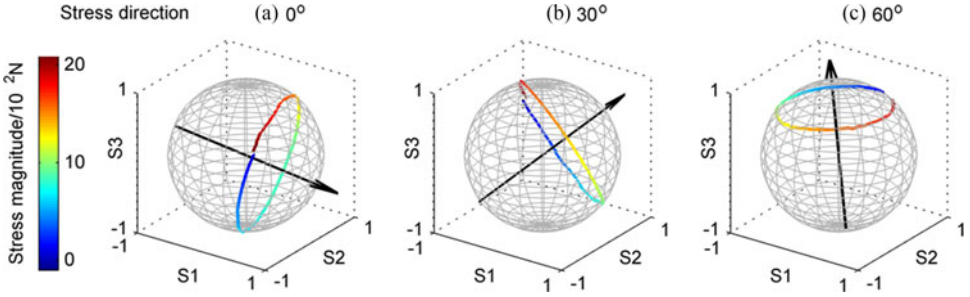

Fig. 7. The FUT is a G.652 SMF, the subfigures respectively show the change of stress principal axis when the direction of external stress changes from 0° to 60°.

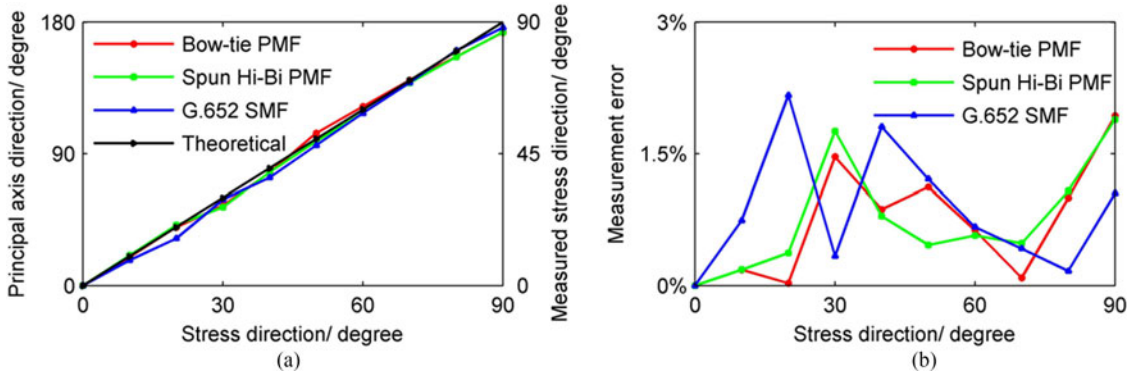

Fig. 8. (a) The measurement of external stress direction based on different types of fibers. (b) The angle measurement error.

measure the external stress direction, originally drawn from the linear Hi-Bi PMF theoretically, can be extended to the other types of fiber. It is worth mentioning that the data required in Figs. 5–7 are the raw data obtained directly from polarization analyzer. These polarization states are plotted in different relative coordinate system when the tested fibers are changed, thus the data need to be calibrated for different tested fiber.

At this stage the linear relation between the stress principal axis and the direction of external stress in optical fiber has been verified theoretically and experimentally, but whether it is accurate enough for practical applications is still unknown. Therefore we apply this method to measure the direction of external stress (from 0° to 90°) by using different fibers based on the experiment setup in Fig. 4. The measurement curves of the external stress direction are depicted in Fig. 8(a), which

show linear behaviors that almost be consistent with the theoretical curve. Fig. 8(b) shows the angle measurement error, and the maximum angle measurement errors are 1.93%, 1.89% and 2.24% based on the bow-tie PMF, Spun Hi-Bi PMF and G.652 SMF respectively. For some kinds of applications this low level of error can be tolerated.

So far the proposed method has been theoretically and experimentally validated based on different types of fiber with low maximum angle measurement errors; however, this technique still need to be improved in several aspect. In fact, the method of measuring the magnitude of external stress based on the SOP's rotation radian is already proposed in 1980 by Smith [28]. Combining these two methods together, it could be employed to measure the magnitude and direction of external stress simultaneously. In addition, the method can only achieve measurement at a single position along the fiber and unable to distinguish the location of external stress so far; while the stress on the fiber (especially the sensitive ring in FOG) are usually random, distributed and more complicated. There is a long way to go from achieving distributed stress measurement and improving the measurement accuracy of FOG by using this method.

4. Conclusion

The birefringence superposition principle is proved theoretically by using the quaternion method. Neglecting the loss of fiber, we studied four factors (i.e., the intrinsic birefringence, the SOP of incident light, the direction and magnitude of external stress) that impact the SOP of the output light in PMF, finally got the linear relationship between the direction of external stress and the stress principal axis. The above linear relationship, in turn, provides a practical method to measure the direction of external stress, with maximum angle measurement errors of less than 2.24% based on different kinds of fiber. In addition, this technique is also feasible to measure the magnitude and direction of external stress simultaneously based on the SOP of the transmission light in theory.

Appendix

In general, the direction of the external stress is not the same as the direction of the principal axis determined by the internal stress, and the angle between them is θ. We first introduce a coordinate system $\xi O \eta$ based on the external stress to analyze the influence of external stress. When a fiber is subjected to external stress, assuming that the longitudinal stress is 0, we only need to consider the stress distribution in the cross-section of fiber core. Thus the dielectric constant induced by external stress is

$$\left[\varepsilon_{\xi,\eta}\right]_{\text{ext}} = \boldsymbol{C}\sigma_{\text{ext}}(x, y, z) = \boldsymbol{C}\begin{bmatrix} \sigma_{\xi\xi} & \sigma_{\xi\eta} \\ \sigma_{\eta\xi} & \sigma_{\eta\eta} \end{bmatrix} \tag{A1}$$

The elastic tensor $\boldsymbol{C}$ is a 9×9 matrix containing 81 components, according to its rotational symmetry, in the coordinate system $\xi O \eta$ we can get

$$\left[\varepsilon'_{\xi,\eta}\right]_{\text{ext}} = \begin{bmatrix} C_1\sigma_{\xi\xi} + C_2\sigma_{\eta\eta} & (C_1 - C_2)\sigma_{\xi\eta} \\ (C_1 - C_2)\sigma_{\xi\eta} & C_1\sigma_{\eta\eta} + C_2\sigma_{\xi\xi} \end{bmatrix} \tag{A2}$$

Where $C_1 = -(n_0^4/E)(P_{11} - 2\nu P_{12})$, $C_2 = -(n_0^4/E)\varepsilon(1 - \nu)P_{12} - 2n_0\nu P_{11}$, E is the Young's modulus, ν is the Poisson's ratio, P_{11} and P_{12} are the elasticity coefficient, n_0 is the refractive index of the fiber in the absence of external stress.

It can be seen from equation (A2), when the external stress is applied, the distribution of the refractive index of the core changes from the initial uniform distribution to the inhomogeneous distribution. In this paper, we use the equivalent step fiber method to calculate the mode field and transmission constant in nonuniformly distributed optical waveguide.

$$\left[\bar{\varepsilon}'_{\xi,\eta}\right]_{\text{ext}} = \begin{bmatrix} C_1\bar{\sigma}_{\xi\xi} + C_2\bar{\sigma}_{\eta\eta} & (C_1 - C_2)\bar{\sigma}_{\xi\eta} \\ (C_1 - C_2)\bar{\sigma}_{\xi\eta} & C_1\bar{\sigma}_{\eta\eta} + \bar{C}_2\sigma_{\xi\xi} \end{bmatrix} \tag{A3}$$

The three stress averages in equation (A3) are defined as:

$$\bar{\sigma}_{\xi\xi} = \frac{1}{\pi a^2}\iint_s \sigma_{\xi\xi}(\xi, \eta)\mathrm{d}s \tag{A4}$$

$$\bar{\sigma}_{\xi\eta} = \frac{1}{\pi a^2}\iint_s \sigma_{\xi\eta}(\xi, \eta)\mathrm{d}s \tag{A5}$$

$$\bar{\sigma}_{\eta\eta} = \frac{1}{\pi a^2}\iint_s \sigma_{\eta\eta}(\xi, \eta)\mathrm{d}s \tag{A6}$$

When the external stress is applied in the direction $O\xi$, the stress distribution in the optical fiber core is

$$\sigma_{\xi\xi} = \frac{P}{\pi R}\frac{-3 + 2\tilde{r}^2[1 + 3\cos(2\phi)]}{1 - 4\tilde{r}^2\cos(2\phi)} \tag{A7}$$

$$\sigma_{\eta\eta} = \frac{P}{\pi R}\frac{1 + 4\tilde{r}^2\cos\phi\cos(3\phi)}{1 - 4\tilde{r}^2\cos(2\phi)} \tag{A8}$$

$$\sigma_{\xi\eta} = \frac{P}{\pi R}\frac{4\tilde{r}^2\sin(2\phi)\{\tilde{r}^2[1 + \cos(2\phi)] - \cos(2\phi)\}}{1 - 4\tilde{r}^2\cos(2\phi)} \tag{A9}$$

Where P is the line pressure (N / m) applied to the optical fiber, R is the outer radius of the optical fiber. $\tilde{r}$ and ϕ are the coordinate of the polar coordinate system with the core as the axis, where $\tilde{r} = r/R$ is the normalized value of the polar coordinate vector.

From the formula (A4)–(A6), the average of the stress depends on the following three integrals

$$I_{\xi\xi} = \iint_{r,\phi}\frac{-3 + 2\tilde{r}^2[1 + 3\cos(2\phi)]}{1 - 4\tilde{r}^2\cos(2\phi)}\tilde{r}\mathrm{d}\tilde{r}\mathrm{d}\phi \tag{A10}$$

$$I_{\eta\eta} = \iint_{r,\phi}\frac{1 + 4\tilde{r}^2\cos\phi\cos(3\phi)}{1 - 4\tilde{r}^2\cos(2\phi)}r\mathrm{d}r\mathrm{d}\phi \tag{A11}$$

$$I_{\xi\eta} = \iint_{r,\phi}\frac{4\tilde{r}^2\sin(2\phi)\{\tilde{r}^2[1 + \cos(2\phi)] - \cos(2\phi)\}}{1 - 4\tilde{r}^2\cos(2\phi)}r\mathrm{d}r\mathrm{d}\phi \tag{A12}$$

Note that these three integrals are independent of the applied stress. For the general PMF $r \in (0,\ 9/125)$, $\varphi \in (0, 2\pi)$, the three integral constants are

$$I_{\xi\xi} = -2.99643,\ I_{\eta\eta} = 1.0008586,\ I_{\xi\eta} \approx 0 \tag{A13}$$

Assuming $\bar{C} = (C_1 + C_2)/2$, $\Delta C = (C_1 - C_2)/2$, then (A3) can be rewritten as

$$\left[\bar{\varepsilon}'_{\xi,\eta}\right]_{\text{ext}} = \begin{bmatrix} \bar{C}(\bar{\sigma}_{\xi\xi} + \bar{\sigma}_{\eta\eta}) + \Delta C(\bar{\sigma}_{\xi\xi} - \bar{\sigma}_{\eta\eta}) & 0 \\ 0 & \bar{C}(\bar{\sigma}_{\xi\xi} + \bar{\sigma}_{\eta\eta}) - \Delta C(\bar{\sigma}_{\xi\xi} - \bar{\sigma}_{\eta\eta}) \end{bmatrix} \tag{A14}$$

Acknowledgment

The authors thank the Beijing Glass Research Institute (BGRI), Yangtze Optical Fiber and Cable Corp (YOFC) and Shanghai Comcore Optical Sensing Technologies Corp for providing different types of fibers.

References

[1] K. Wada, H. Narui, D. Yamamoto, T. Matsuyama, and H. Horinaka, "Balanced polarization maintaining fiber Sagnac interferometer vibration sensor," *Opt. Exp.*, vol. 19, no. 22, pp. 21467–21474, 2011.

[2] Z. Qin, T. Zhu, L. Chen, and X. Bao, "High sensitivity distributed vibration sensor based on polarization-maintaining configurations of phase-OTDR," *IEEE Photon. Technol. Lett.* vol. 23, no. 15, pp. 1091–1093, Aug. 2011.

[3] Y. Tong *et al.*, "Distributed incomplete polarization-OTDR based on polarization maintaining fiber for multi-event detection," *Opt. Commun.*, vol. 357, pp. 41–44, 2015.

[4] J. Zhang *et al.*, "Highly sensitive temperature sensor using PANDA fiber Sagnac interferometer," *J. Lightw. Technol.*, vol. 29, no. 24, pp. 3640–3644, Dec. 2011.
[5] M. A. Soto, X. Lu, H. F. Martins, M. Gonzalez-Herraez, and L. Thévenaz, "Distributed phase birefringence measurements based on polarization correlation in phase-sensitive optical time-domain reflectometers," *Opt. Exp.*, vol. 23, no. 19, pp. 24923–24936, 2015.
[6] Z. Li *et al.*, "Complete characterization of polarization-maintaining fibers using distributed polarization analysis," *J. Lightw. Technol.*, vol. 33, no. 2, pp. 372–380, Jan. 2015.
[7] H. Wang, F. Tu, J. Li, H. Wei, and S. Song, "Effect of temperature and bending on PANDA polarization-maintaining fibers fabricated by PCVD method," in *Proc. IEEE PhotonicsGlobal@ Singapore*, 2008, pp. 1–4.
[8] Z. Ou *et al.*, "The research on beat length of polarization maintaining optical fiber with external pressure," *Optik: Int. J. Light Electron Opt.*, vol. 125, no. 20, pp. 6058–6062, 2014.
[9] R. Ulrich, S. C. Rashleigh, and W. Eickhoff, "Bending-induced birefringence in single-mode fibers," *Opt. Lett.*, vol. 5, no. 6, pp. 273–275, 1980.
[10] S. Rashleigh, "Origins and control of polarization effects in single-mode fibers," *J. Lightw. Technol.*, vol. JLT-1, no. 2, pp. 312–331, Jun. 1983.
[11] P. Chu and R. Sammut, "Analytical method for calculation of stresses and material birefringence in polarization-maintaining optical fiber," *J. Lightw. Technol.*, vol. JLT-2, no. 5, pp. 650–662, Oct. 1984.
[12] M. Tsubokawa, T. Higashi, and Y. Negishi, "Mode couplings due to external forces distributed along a polarization-maintaining fiber: An evaluation," *Appl. Opt.*, vol. 27, no. 1, pp. 166–173, 1988.
[13] R. Ulrich and A. Simon, "Polarization optics of twisted single-mode fibers," *Appl. Opt.*, vol. 18, no. 13, pp. 2241–2251, 1979.
[14] R. Ulrich and M. Johnson, "Single-mode fiber-optical polarization rotator," *Appl. Opt.*, vol. 18, no. 11, pp. 1857–1861, 1979.
[15] S. C. Rashleigh and R. Ulrich, "Magneto-optic current sensing with birefringent fibers," *Appl. Phys. Lett.*, vol. 34, no. 11, pp. 768–770, 1979.
[16] I. P. Kaminow and V. Ramaswamy, "Single-polarization optical fibers: Slab model," *Appl. Phys. Lett.*, vol. 34, no. 4, pp. 268–270, 1979.
[17] V. Ramaswamy, W. G. French, and R. D. Standley, "Polarization characteristics of noncircular core single-mode fibers," *Appl. Opt.*, vol. 17, no. 18, pp. 3014–3017, 1978.
[18] O. Katsunari, T. Hosaka, and T. Edahiro, "Stress analysis of optical fibers by a finite element method," *IEEE J. Quantum Electron.*, vol. QE-17, no. 10, pp. 2123–2129, Oct. 1981.
[19] W. Eickhoff, "Stress-induced single-polarization single-mode fiber," *Opt. Lett.*, vol. 7, no. 12, pp. 629–631, 1982.
[20] K. Y. Song, "High-sensitivity optical time-domain reflectometry based on Brillouin dynamic gratings in polarization maintaining fibers," *Opt. Exp.*, vol. 20, no. 25, pp. 27377–27383, 2012.
[21] H. Y. Fu *et al.*, "Pressure sensor realized with polarization-maintaining photonic crystal fiber-based Sagnac interferometer," *Appl. Opt.*, vol. 47, no. 15, pp. 2835–2839, 2008.
[22] O. Jose, E Beckert, T. Burkhardt, M Hornaff, and A. Kamm, "Experimental evaluation of the polarization crosstalk when soldering a polarization-maintaining fiber into a V-grooved substrate," *IEEE Trans. Compon., Packag., Manuf. Technol.*, vol. 3, no. 4, pp. 543–548, Apr. 2013.
[23] A. M. Smith, "Single-mode fibre pressure sensitivity," *Electron. Lett.*, vol. 16, no. 20, pp. 773–774, 1980.
[24] M. Karlsson and M. Petersson, "Quaternion approach to PMD and PDL phenomena in optical fiber systems," *J. Lightw. Technol.*, vol. 22, no. 4, pp. 1137–1146, Apr. 2004.
[25] D. Guangtao, "Quaternion method in polarization optics," *Acta Opt. Sin.*, vol. 33, no. 7, 2013, Art. no. 0726001 (in Chinese).
[26] L. Liu and C. Wu, "Investigation of polarization state generation with ergodicity of polarization states based on the quaternion approach," *Acta Opt. Sin.*, vol. 34, no. 3, pp. 0306002-1–0306002-5, 2014 (in Chinese).
[27] L. Liu, C. Wu, C. Shang, Z. Li, and J. Wang, "Quaternion approach to the measurement of the local birefringence distribution in optical fibers," *IEEE Photon. J.*, vol. 7, no. 4, Aug. 2015, Art. no. 6901014.
[28] R. Ulrich, "Polarization stabilization on single-mode fiber," *Appl. Phys. Lett.*, vol. 35, no. 11, pp. 840–842, 1979.
[29] G. N. Ramachandran and S. Ramaseshan, "Crystal optics," in *Handbuch der Physik*, S. Flugge, Ed. Berlin, Germany: Springer, 1961, vol. 25/1, p. 1.